

Orbit response matrix method applied to SIS18 for lattice optimization

A. Parfenova, G. Franchetti, C. Omet
 GSI, 64291 Darmstadt, Germany

S.Y. Lee
 Indiana University, Bloomington, IN 47405, USA

May 24, 2007

The Orbit Response Matrix (ORM) method was applied to model the GSI heavy ion synchrotron SIS18. Using the horizontal and vertical closed orbit (CO) data we are able to calibrate 18 steerers (6 horizontal and 12 vertical), 24 BPMs (12 horizontal and 12 vertical) and 24 quadrupole gradients (12 horizontal and 12 vertical). We present the results of several measurements done in February-April 2006 and discuss the achieved improvement of the SIS18 performance. Problems associated with the experiment and the modelling will be also considered.

1 Introduction

The SIS18 will be used as a booster for the new SIS100 of the FAIR project. A well-controlled linear optics of the SIS18 is necessary for further optimization studies of nonlinear dynamics, resonance induced beam loss [1], dynamic aperture and nonlinear error measurements. The analysis of the orbit response matrix (ORM) is a powerful tool to calibrate the linear lattice models [2].

Every BPM/steerer has a calibration factor, which is defined as the ratio between ‘given’ and ‘outcome’ position/angle values, see Fig. 1 top. For the ideally calibrated BPM/steerer the ratio between ‘given’ to ‘outcome’ position/angle is 1. Another way to explain it is to consider the linear beam position response to a small change in steerer angle, see Fig. 1 bottom: it can be simulated a) as well as measured b). The experimental angle and beam position are related to model ones via $\theta_{exp} = \theta_{model} f$, $x_{exp} = x_{model} g$, where g and f are BPM and steerer calibration factors respectively. In the ideal case $g = 1$ and $f = 1$ so that experiment and model coincide ($\theta_{exp} = \theta_{model}$, $x_{exp} = x_{model}$). The experimental slope α_{exp} can be expressed through the model slope α_{model} as

$$\alpha_{exp} = \frac{x_{exp}}{\theta_{exp}} = \frac{x_{model} g}{\theta_{model} f} = \alpha_{model} \frac{g}{f}. \quad (1)$$

The factors g and f connect the ‘given’ α_{model} and the ‘outcome’ α_{exp} . To find how the calibration of each BPM and steerer differs from 1 we use the ORM analysis.

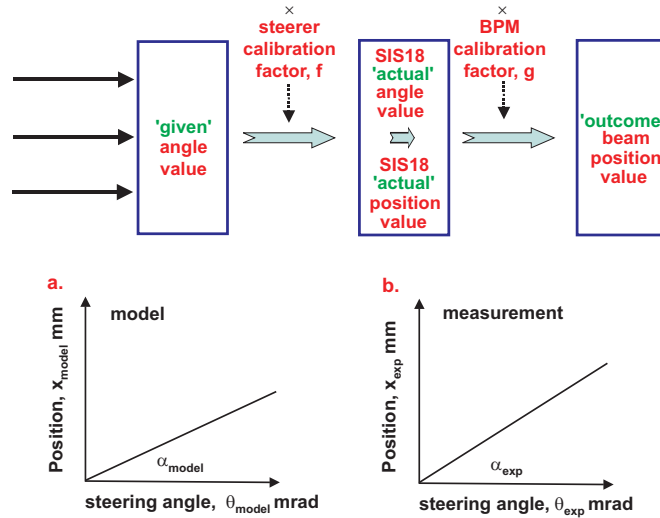


Figure 1: Top) schematic description of calibration factor; bottom) model and measurement dependence of beam position on steering angle.

In May 2006 the SIS18 CO was corrected for the injection and extraction energies. The CO correction at injection is presented on Fig. 2 a). The correction was based on the three-steerer local bump method [3, 4, 5]. In December 2006, a semi-automatic CO correction based on this method was implemented into the SIS18 control program [6]. The local bump is provided by a certain ratio between three steering angles of three neighbour steerers [5]. To hold precisely this ratio in the measurement ‘well’ calibrated steerers are required [3]. ‘Well’ calibrated means that all the steerers have the same calibration factors, which are equal to 1.0.

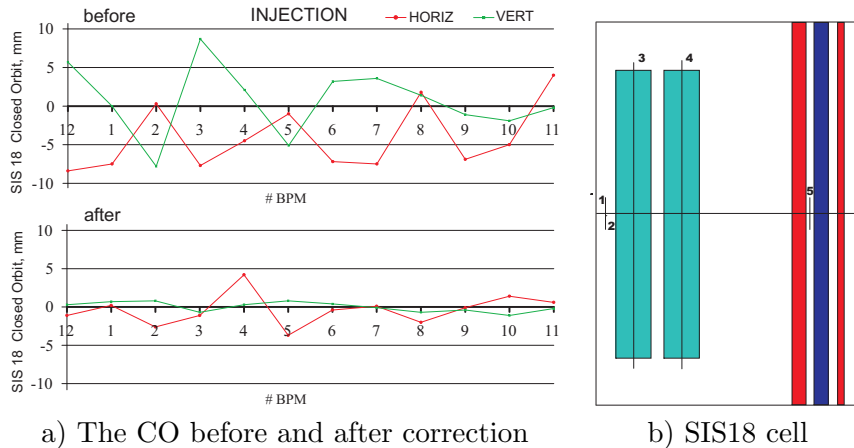


Figure 2: a) The horizontal and vertical CO at injection energy before (top) and after (bottom) the CO correction; b) One SIS18 cell: 1,2 - horizontal and vertical BPMs; 3,4 - horizontal steerers located in first/second dipoles; 5 - vertical steerer; dipoles (light blue), focusing quadrupoles (red) and defocusing quadrupoles (blue).

In Fig. 3 an example of ‘well’ a) and ‘wrong’ b) steerer calibration measured in the

SIS18 is shown. The BPM #8 (S08DX) is absent in the measurement. If the calibration factors of all three steerers are equal then the ratio between the three steerer angles is fulfilled and the ‘perfect’ local bump is possible, see Fig. 3 a). In this case the CO distortion is localized between BPMs #1 (S01DX) and #3 (S03DX), which are in the same periods with the steerers #1 (S01KM2DV) and #3 (S03KM2DV) [4]. If the calibration factors of the steerers are unequal then the local bump is ‘imperfect’ and CO is globally distorted, see Fig. 3 b). To perform the CO correction in an optimal way, a calibration of the steerers and BPMs has to be carried out.

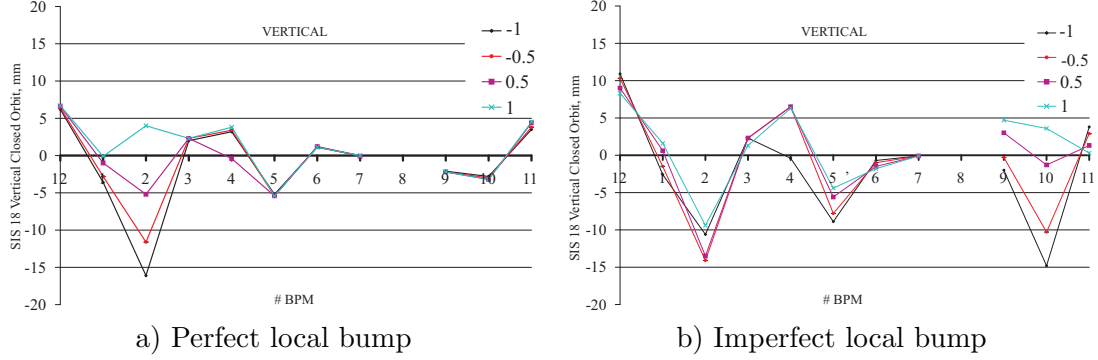


Figure 3: Local vertical CO distortion of different strength measured at 12 BPMs in POSI [17] created by the three vertical steerers (black curve - $\theta_1 = -1.0$ mrad; red curve - $\theta_1 = -0.5$ mrad; magenta curve - $\theta_1 = 0.5$ mrad; blue curve - $\theta_1 = 1.0$ mrad): a) using #1 (S01KM2DV), #2 (S02KM2DV), #3 (S03KM2DV) steerers; b) using #9 (S09KM2DV), #10 (S10KM2DV), #11 (S11KM2DV) steerers.

The SIS18 has 12 periods and a nominal working point at injection energy of $Q = (4.29; 3.29)$. There are 24 beam position monitors (BPMs) by 12 in each plane used for the CO diagnostics [7]. For CO control and correction 6 horizontal and 12 vertical steerers are available. The vertical steerers are independent steering magnets, while the horizontal steerers are made of extra coils in dipoles, which have unipolar power supplies [8]. The names of BPMs and steerers are found in Table 1. In the SIS18, 24 dipole magnets are used for the beam bending. The dipoles are connected into one family, i.e. powered in series from the same power supply. For focusing of the beam there are 24 horizontal focusing quadrupoles and 12 vertical focusing (horizontal defocusing) quadrupoles. The quadrupoles are united in five families [8], which are listed in Table 2. The 24 focusing quadrupoles form two families by six (Q1F and Q2F) and one family by 12 magnets (Q1T). The 12 defocusing quadrupoles form two families by six magnets (Q1D and Q2D). In Fig. 2 b) the BPM- and steerer-, dipole- and quadrupole- locations for one SIS18 cell are shown.

2 Analytical model

The orbit response matrix gives a change in closed orbit \mathbf{x}_{co} , \mathbf{y}_{co} by change in steerer angles θ_x , θ_y [11]

$$\begin{pmatrix} \mathbf{x}_{co} \\ \mathbf{y}_{co} \end{pmatrix} = \mathbf{M}_{orm} \begin{pmatrix} \theta_x \\ \theta_y \end{pmatrix}, \quad (2)$$

where \mathbf{M}_{orm} is either the measured or model response matrix, $\mathbf{x}_{co} = (x_{co,1} x_{co,2} \dots)$, $\mathbf{y}_{co} = (y_{co,1} y_{co,2} \dots)$, $\theta_x = (\theta_{x,1} \theta_{x,2} \dots)$, $\theta_y = (\theta_{y,1} \theta_{y,2} \dots)$ and the indices 1, 2, 3... are the

Table 1: SIS18 steerers and BPMs used in the ORM measurements.

Vertical steerers (bipolar)	Horizontal steerers (unipolar)	BPMs horizontal and vertical
S01KM2DV, S02KM2DV	S01MU1A (positive)	S01DX, S02DX
S03KM2DV, S04KM2DV	S03MU1A (positive)	S03DX, S04DX
S05KM2DV, S06KM2DV	S05MU1A (negative)	S05DX, S06DX
S07KM2DV, S08KM2DV	S06MU2A (negative)	S07DX, S08DX
S09KM2DV, S10KM2DV	S09MU1A (negative)	S09DX, S10DX
S11KM2DV, S12KM2DV	S12MU1A (positive)	S11DX, S12DX

Table 2: Quadrupole families of the SIS18.

Q1F focusing	Q2F focusing	Q1D defocusing	Q2D defocusing	Q1T focusing
S01QS1F	S02QS1F	S01QS2D	S02QS2D	S01QS3T, S02QS3T
S03QS1F	S04QS1F	S03QS2D	S04QS2D	S03QS3T, S04QS3T
S05QS1F	S06QS1F	S05QS2D	S06QS2D	S05QS3T, S06QS3T
S07QS1F	S08QS1F	S07QS2D	S08QS2D	S07QS3T, S08QS3T
S09QS1F	S10QS1F	S09QS2D	S10QS2D	S09QS3T, S10QS3T
S11QS1F	S12QS1F	S11QS2D	S12QS2D	S11QS3T, S12QS3T

BPMs and steerer sequence as found in the ring. Theoretically, the elements of the orbit response matrix are given by the Green's function:

$$M_{ij} = G(s_i, s_j) = \frac{\sqrt{\beta(s_i)\beta(s_j)}}{2 \sin(\pi\nu)} \cos(\pi\nu - |\psi(s_i) - \psi(s_j)|), \quad (3)$$

where s_i, s_j are the positions of the i th BPM and the j th steerer; $\beta(s_i)$ and $\beta(s_j)$ are the β -functions at these locations; $\psi(s_i), \psi(s_j)$ are the phase-advances, ν stands for the tune.

Now we define the following model parameters (variables)

- BPM calibration factors $\mathbf{g} = \{g_i\}$, $i = 1 \dots I$, I is the total number of BPMs,
- steerer calibration factors $\mathbf{f} = \{f_j\}$, $j = 1 \dots J$, J is the total number of steerers,
- quadrupole gradients $\mathbf{q} = \{q_l\}$, $l = 1 \dots L$, L is the total number of quadrupoles,

which form the model/fit parameters' vector $\mathbf{x} = (\mathbf{g}, \mathbf{f}, \mathbf{q}) = \{x_m\}$, $m = 1 \dots M$, $M = I + J + L$ is the total number of model parameters.

To minimize the difference between the model \mathbf{M}^{mod} and measured \mathbf{M}^{exp} orbit response matrices, the vector $V_n = (M_{ij}^{\text{mod}} - M_{ij}^{\text{exp}})/\sigma_{ij}$ is defined, where we have ordered the components ij of the matrix into a vector of n components. The index n runs over all the data points and is formed by multiplication of the number of steerers varied j and the number of BPMs used i . Each n corresponds to a precise value of ij , that is $n \rightarrow (\bar{i}, \bar{j})$. The total number of fitting data points is $N = I \times J$. The weighting factor σ_{ij} (rms uncertainty of the measurement in each point) gives more weight to those measured ORM elements with lower noise. The measured matrix always includes the BPM and steerer calibration factors and can be derived via $M_{ij}^{\text{exp}} = M_{ij}^{\text{data}}/(g_i f_j)$. The χ^2 -function is a function which used in statistics to express how much a theoretical

model differs statistically from experimental data [9, 10]. The following χ^2 -function is introduced as a measure of difference between \mathbf{M}^{mod} and \mathbf{M}^{exp} and has to be minimized:

$$\chi^2 = \sum_n V_n^2 = \sum_n \frac{(M_{i\bar{j}}^{\text{mod}} - M_{i\bar{j}}^{\text{data}} / (g_i f_{\bar{j}}))^2}{\sigma_{i\bar{j}}^2}. \quad (4)$$

The multi-dimensional non-linear least-square problem (4), i.e. the minimization of χ^2 , can be solved by varying the model parameter vector \mathbf{x} , which are quadrupole gradients \mathbf{q} , steerer calibration factors \mathbf{f} and BPM calibration factors \mathbf{g} . The variation of the V_n th component due to the variation of the m -th component of \mathbf{x} is found [10]

$$V_n(\mathbf{x} + \Delta\mathbf{x}) \approx V_n(\mathbf{x}) + \sum_m \frac{\partial V_n}{\partial x_m} \cdot \Delta x_m. \quad (5)$$

Imposing Equation (5) to zero we find an approximate solution by multi-dimensional Newton method and build iterative process

$$V_n(\mathbf{x}) + \sum_m \frac{\partial V_n}{\partial x_m} \cdot \Delta x_m = 0. \quad (6)$$

The Jacobian \mathbf{J} of the linear system Equations (6) consists of all partial derivatives of the parameters

$$J_{nm} = \frac{\partial V_n}{\partial x_m}. \quad (7)$$

Equation (6) is called the normal equation of the least-square problem [10] and can be rewritten in the following way

$$\mathbf{V} + \mathbf{J}\Delta\mathbf{x} = 0. \quad (8)$$

By iteratively solving the linear Equation (8) for all the $\Delta\mathbf{x}$, χ^2 can be minimized and the vector of model parameters \mathbf{x} for the best fitted model can be obtained.

2.1 Jacobian calculation

The Jacobian (7) is formed by sub-Jacobians for every group of parameters. The sub-Jacobians for steerer and BPM calibration factors are dependent on the measured matrix

$$(J^g)_{ni} = \frac{\partial V_n}{\partial g_i} = \begin{cases} 0, & \text{if } i \neq \bar{i} \\ \frac{M_{i\bar{j}}^{\text{data}}}{\sigma_{i\bar{j}}^2 g_i f_{\bar{j}}}, & \text{if } i = \bar{i}, \end{cases} \quad (9)$$

$$(J^f)_{nj} = \frac{\partial V_n}{\partial f_j} = \begin{cases} 0, & \text{if } j \neq \bar{j} \\ \frac{M_{i\bar{j}}^{\text{data}}}{\sigma_{i\bar{j}}^2 g_i f_j^2}, & \text{if } j = \bar{j}, \end{cases} \quad (10)$$

The sub-Jacobian for quadrupole gradient strength errors is dependent on the model matrix

$$(J^q)_{nl} = \frac{\partial V_n}{\partial q_l} = \frac{M_{i\bar{j}}^{\text{mod}}(\mathbf{q} + \epsilon \hat{\mathbf{v}}) - M_{i\bar{j}}^{\text{mod}ij}(\mathbf{q})}{\sigma_{i\bar{j}}^2 \epsilon}. \quad (11)$$

The Equation (8) in terms of sub-Jacobians could be rewritten as

$$\mathbf{V} + \mathbf{J}^q \Delta\mathbf{q} + \mathbf{J}^g \Delta\mathbf{g} + \mathbf{J}^f \Delta\mathbf{f} = 0. \quad (12)$$

Note that the sub-Jacobians \mathbf{J}^f and \mathbf{J}^g are correlated. It is not possible independently to vary all the BPM calibrations \mathbf{g} and all steerer calibrations \mathbf{f} , because there is a degeneracy in the solution of Equation (8) [11], [12]. All the BPM calibrations could be increased while all the steerer calibrations were decreased ($g/f = \text{const}$), and the model matrix would stay constant. It is seen as well from the definition of BPM and steerer calibration factors, see Equation (12). The degeneracy leads to zero eigenvalue in matrix $\mathbf{J}^T \mathbf{J}$ [10]. The inclusion of the dispersion function into the orbit response matrix would decouple BPM and steerer calibration factors, so that the degeneracy could be avoided. This can be done by extending the orbit response matrix by one more column that consists of dispersion terms [2, 11, 12]. Another way to avoid the degeneracy is to assume that one horizontal and one vertical corrector were calibrated correctly (calibration factor 1). Therefore in the ORM modelling two steerer strengths (one horizontal and one vertical) are kept fixed, and all the other steerers and BPMs were calibrated relative to these two steerers.

2.2 Solving the system of linear equations: Singular Value Decomposition method

There exists a very powerful set of techniques for dealing with sets of equations or matrices that are either singular or else numerically very close to singular. The small eigenvalues might be generated by noise in data, random errors or non-essential accelerator parameters. In many such cases where Gaussian elimination [10] fails to give satisfactory results, this set of techniques, known as singular value decomposition or SVD [10].

In our case the least-square problem is overdetermined if the number of data points N would be greater than the number of parameters M . For this case SVD gives a solution with the minimum norm that is the best approximation in the least-square sense (so called residual solution). So that according to SVD method Jacobian matrix Equation (7) can be written as a product

$$\mathbf{J} = \mathbf{U} \mathbf{\Lambda} \mathbf{Q}^T, \quad (13)$$

where \mathbf{U} , \mathbf{Q} are orthogonal matrices, $\mathbf{\Lambda}$ is a diagonal matrix consists of eigenvalues of matrix $\mathbf{J}^T \mathbf{J}$. The solution (the change in model parameter vector \mathbf{x}) in one iteration is performed via pseudoinverse of the decomposed Jacobian \mathbf{J}

$$\Delta \mathbf{x} = -\mathbf{J}^{-1} \mathbf{V} = -\mathbf{Q} \mathbf{\Lambda}^{-1} \mathbf{U}^T \mathbf{V}. \quad (14)$$

The model parameter vector \mathbf{x} on the $k + 1$ iteration is defined as

$$\mathbf{x}^{k+1} = \mathbf{x}^k - \mathbf{J}^{-1}(\mathbf{x}^k) \mathbf{V}(\mathbf{x}^k). \quad (15)$$

The new value \mathbf{x}^{k+1} has to satisfy the χ^2 -convergence condition: $\chi_{k+1}^2 < \chi_k^2$. By iterating till the desired χ^2 -tolerance is reached, the fitted model can be obtained. Practically the iterations can be stopped when an extra iteration makes only a small change to χ^2 .

However, a very common situation is that some of the eigenvalues of matrix $\mathbf{J}^T \mathbf{J}$ are very small but nonzero, so that the matrix is ill-conditioned [10]. Some of the small eigenvalues might correspond to noise and measurement errors in experimental data. In that case SVD is needed to set a tolerance level (to cut-off small eigenvalues) to

obtain a satisfactory results: set the inverse of all eigenvalues to zero if they are smaller than a cut-off threshold called the tolerance level. This procedure corresponds to throw away one linear combination of the set of equations that we are trying to solve. Usually throwing away a combination of equations, ‘pulls’ the solution vector away off towards infinity along some direction that is almost a nullspace vector [10]. In doing this, it compounds the roundoff problem and makes the residual $|\mathbf{J}\Delta\mathbf{x} - \mathbf{V}|$ larger. As small eigenvalues can have a big contribution into the solution, SVD can not be applied blindly. The choice of the tolerance level for SVD in experimental data analysis is a very delicate task: cutting out too many eigenvalues will make the solution space incomplete and solution will suffer, leaving in too many small eigenvalues will make the solution unstable.

2.3 Solving the system of linear equations: Levenberg-Marquardt method

Levenberg-Marquardt is another method, which is very well used in practice and has become the standard of nonlinear least-squares routines. Levenberg-Marquardt is more robust than SVD in dealing with small eigenvalues: it does not need the use of any tolerance level. Instead of solving the linear system Equation (8) with Jacobian (7) the following equation is solved [10]

$$(\mathbf{J}^T\mathbf{J} + \lambda\mathbf{I})\Delta\mathbf{x} = -\mathbf{J}^T\mathbf{V}, \quad (16)$$

where \mathbf{I} is the identity matrix, λ is an adjustable parameter, which belongs to the interval $[0, 1]$. At every iteration the parameter λ is adjusted to satisfy the χ^2 -convergence condition: $\chi_{k+1}^2 < \chi_k^2$. The parameter vector on the next iteration is defined as $\mathbf{x}^{k+1} = \mathbf{x}^k + \Delta\mathbf{x}$.

The recommended Levenberg-Marquardt algorithm is the following [10]:

- Compute $\chi^2(\mathbf{x})$;
- Pick a modest value for λ , say $\lambda = 0.001$;
- (†) Solve Equation (16) for $\Delta\mathbf{x}$ and evaluate $\chi^2(\mathbf{x} + \Delta\mathbf{x})$;
- If $\chi^2(\mathbf{x} + \Delta\mathbf{x}) \geq \chi^2(\mathbf{x})$, *increase* λ by a factor of 10 (or any other substantial factor) and go back to (†);
- If $\chi^2(\mathbf{x} + \Delta\mathbf{x}) < \chi^2(\mathbf{x})$, *decrease* λ by a factor of 10, update the trial solution $\mathbf{x} \leftarrow \mathbf{x} + \Delta\mathbf{x}$, and go back to (†).

According to the above algorithm χ^2 converges to the solution while the parameter λ converges to zero [10]: $\lim_{\lambda \rightarrow 0} \chi^2 \rightarrow 0$, so that Equations (16) and (14) have the same solution [10].

Note that Levenberg-Marquardt is faster than SVD as the matrix on the left hand side of Equation (16) has smaller dimension. SVD requires an extra array of size $N \times M$ to store the whole matrix \mathbf{J} .

2.4 ORM test simulations

The orbit response matrix fitting program was written on script languages BASH and AWK [13], combined with Scilab [14] and MAD [15]. MAD was used to perform linear

optics calculations of the SIS18, Scilab has been used in mathematical part of calculation, AWK was applied to acquisition of experimental data files and BASH was used as a main tool for external execution. The fitting program has an option to calculate ORM with SVD method as well as with Levenberg-Marquardt. For SVD calculation it is possible to set a tolerance level if needed.

Many simulations have been done to confirm that the fit parameter values \mathbf{x} produced by the code accurately predict the SIS18 lattice. The above fitting scheme was applied to the simulated noise-free horizontal $\mathbf{M}_{xx}^{\text{mad}}$ and vertical ORM $\mathbf{M}_{yy}^{\text{mad}}$. The noise-free means that all σ_{ij} are equal to 1.0. The model ORMs were generated by MAD [15] for SIS18 lattice by introducing random quadrupole errors. In case of vertical ORM $\mathbf{M}_{yy}^{\text{mad}}$ 12 quadrupole random errors within maximum 5% deviation of the nominal value have been introduced. For the horizontal ORM $\mathbf{M}_{xx}^{\text{mad}}$ 24 quadrupole random errors within 5% deviation of the nominal value have been chosen. The matrices were multiplied by a certain random factor out of the interval [0.9; 1.2] to simulate ‘wrong’ BPM and steerer calibration. The horizontal $\mathbf{M}_{xx}^{\text{mad}}$ and vertical $\mathbf{M}_{yy}^{\text{mad}}$ (as well as their χ^2) were functions of random BPM calibration factors, random steerer calibration factors and quadrupole gradients. The actual values of the quadrupole gradients shown in Table 3, were take as initial conditions (starting values for quadrupole gradients in the fit). The initial BPM and steerer calibration factors were set to value 1.0.

Table 3: Used in the SIS18 present lattice model values of the quadrupole gradients, united into families.

Quad. family	Nominal quad. grad., (m^{-2})
Q1F	0.30989596
Q2F	0.30989596
Q1D	-0.49964116
Q2D	-0.49964116
Q1T	0.62221964

The vertical $\mathbf{M}_{yy}^{\text{mad}}$ was a function of 12 known random BPM calibration factors, 12 known random steerer calibration factors and 12 known random quadrupole gradients (quadrupole families Q1D and Q2D). The solution \mathbf{x} (12 BPM calibrations, 12 steerer calibrations and 12 quadrupole gradients) for $\mathbf{M}_{yy}^{\text{mad}}$ does exist, is known and unique. The simultaneous fit of all the parameters was performed with SVD method (without tolerance level) and with Levenberg-Marquardt method. It was found that the two methods converge to the same result: χ^2 monotonously converges to 0 with any desirable accuracy and the solution \mathbf{x} that is the given random error set of model parameters is reconstructed. The convergence of the vertical χ^2 is presented on Fig. 4 a).

In horizontal model ORM $\mathbf{M}_{xx}^{\text{mad}}$ 12 known random BPM calibration factors, 6 known random steerer calibration factors and 24 known random quadrupole gradients (quadrupole families Q1F, Q2F and Q1T) were varied. Note that for the horizontal ORM simulations only 6 steerers were taken because only 6 horizontal steerers are available in the SIS18. The convergence of the horizontal χ^2 is shown on Fig. 4 b). SVD (without tolerance) and Levenberg-Marquardt methods converged to the same result for the model $\mathbf{M}_{xx}^{\text{mad}}$ fit. Note that to measure the horizontal CO for the tune $Q_x = 4.29$, the minimum number of BPMs has to be equal to $3 \times 4 = 12$, where 4 is the integer number of betatron oscillations multiplied by 3 [16]. It has been checked that when less than 12 BPMs are used in the simulations of the horizontal ORM, then a unique solution is

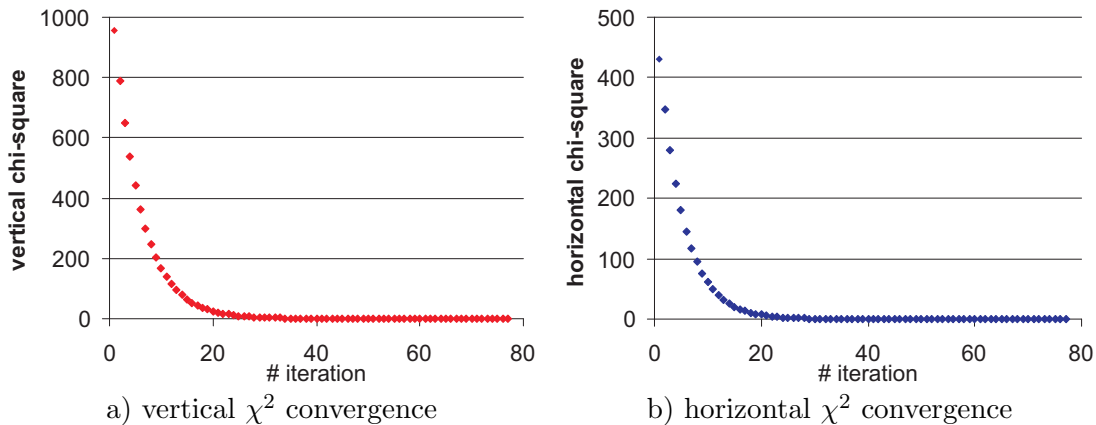


Figure 4: χ^2 vs. number of iterations for the noise-free simulated vertical $\mathbf{M}_{yy}^{\text{mad}}$ a) and horizontal $\mathbf{M}_{xx}^{\text{mad}}$ b), calculation by Levenberg-Marquardt method.

not found. By using minimum 12 BPMs is only possible to resolve the problem with 24 randomly varied quadrupole gradients (1 BPM for 2 magnets). In the case of less BPMs, the algorithm reduces the χ^2 down to zero efficiently but it does not converge to the expected solution. To solve this problem either the number of quadrupoles has to be reduced or the number of BPMs increased till at least to 12.

3 The Orbit Response Matrix Experiment

To get the ORM several measurement campaigns in the SIS18 were performed in February-April 2006. All measurements were taken with different ions, energies and tunes. The multiturn injection was set to fill SIS18 acceptance. The order of intensity and injection energy were kept nearly constant, see Table 4. A medium intensity level of 10^9 particles was required in order to exclude the influence of space charge on the beam position for the ORM measurement. The SIS18 ORM was measured in both planes (horizontal and vertical). In order to have statistical information and perform the best fit, the orbit response matrix was measured three times [11].

Table 4: The ORM measurement campaigns in February-April 2006.

ORM measurement	Ion	Injection energy, MeV/u	Operating tunes	Order of intensity	Missing BPMs
February 28	$^{107}\text{Ag}^{43+}$	11.165	(3.29;4.29)	10^9	#3, #7 horiz., #7, #8 vert.
April 8	$^{86}\text{Kr}^{34+}$	11.241	(3.29;4.29)	10^9	#11 vert.
April 20	$^{40}\text{Ar}^{18+}$	11.380	(4.17;3.35)	10^9	#11 vert.

The ORM was measured by means of the POSI program [17]. POSI reads the beam position data from all position pick-ups and provides automatically the average CO over many synchrotron turns for each pickup. The accuracy of a beam position measurement, defined as a statistical error of a single measurement is ± 0.5 mm in horizontal and ± 0.14 mm in vertical plane respectively. Note that the horizontal accuracy of ± 0.5 mm is ~ 3 times poorer than the vertical of ± 0.14 mm. This accuracy is determined

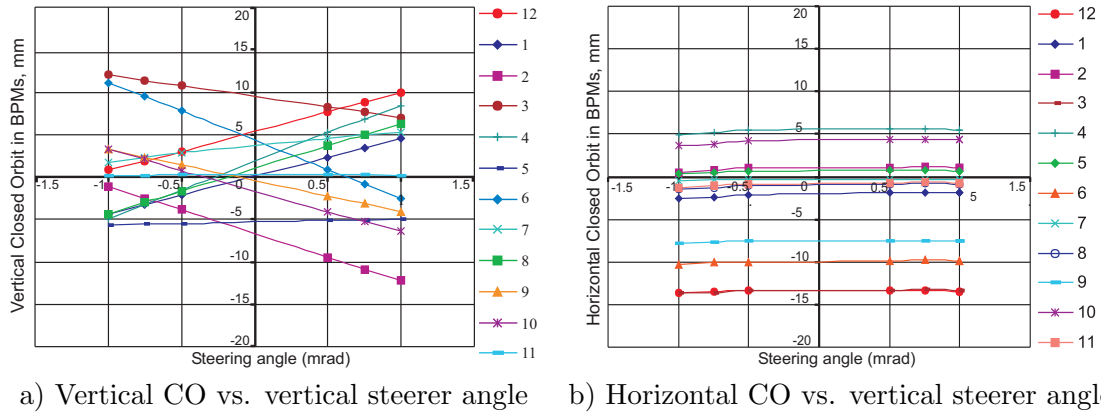


Figure 5: a) Vertical (M_{yy}) and b) horizontal (M_{xy}) closed orbit displacement vs. vertical steering angle. Dots are the measurement values. The solid lines represent the linear fits. Number of every color line corresponds to number of BPM.

by the ADC resolution, thermal noise of the preamplifier and digitalization noise. Both noise sources have stochastic character, whereas the noise caused by the digitalization is dominant. The averaging over many turns improves the precision of the position measurement by the cancelling the stochastic noise. The thermal noise is reduced by using the narrowband analysis [19]. The averaging over many turns increases the accuracy of the position measurement, but it can be used only as long as the beam parameters remain constant. Otherwise, the changes of the beam parameters enter as systematic error in the position measurement accuracy [20].

The ORM is given by the linear fit to the closed orbit vs. the steerer angle. The slopes of the lines in Fig. 5 form the ORM and their standard deviations form the rms uncertainty matrix σ_{ij} . The best accuracy of the ORM achieved in the fit is 0.02 mm/mrad. The maximum deviation from the linear fit is 0.9 mm/mrad. Note that the larger the amplitude of the shifted orbit, the better the signal to noise ratio. The maximum beam amplitude is limited by the machine nonlinearities: the kick angle should not be too strong. We find that within 1.5 mrad the response is still linear, which corresponds to a CO shift ~ 1.5 cm, Fig. 5 a).

The linear optics errors (fit/model parameters) considered here are: steering magnet and BPM calibration factors and quadrupole gradients. The linear coupling errors were not considered and they contribute to systematic errors of the considered fit parameters. In the model as well as in the measurement the complete response matrix \mathbf{M}_{orm} is

$$\mathbf{M}_{orm} = \begin{pmatrix} \mathbf{M}_{xx} & \mathbf{M}_{xy} \\ \mathbf{M}_{yx} & \mathbf{M}_{yy} \end{pmatrix} \quad (17)$$

where \mathbf{M}_{xx} is the horizontal response to horizontal steerers, \mathbf{M}_{xy} is the horizontal response to vertical steerers, etc... No coupling fit means that \mathbf{M}_{xx} and \mathbf{M}_{yy} are considered separately. The measurements were performed in conditions to reduce the impact of linear coupling. The condition of linear coupling $Q_x - Q_y = 1$ for the measured tunes is not satisfied, in fact we find $Q_x - Q_y = 1.05$ (February 28, April 8) and $Q_x - Q_y = 0.87$ (April 20). Comparing with previous measurements the value 1.05 is at the edge of the linear-coupling resonance stop-band [21]. In all three measurements it has also been checked that a kick in vertical direction has no horizontal orbit response (no impact on horizontal BPMs), from which we conclude that $\mathbf{M}_{xy} = 0$ and $\mathbf{M}_{yx} = 0$,



Fig. 5 b).

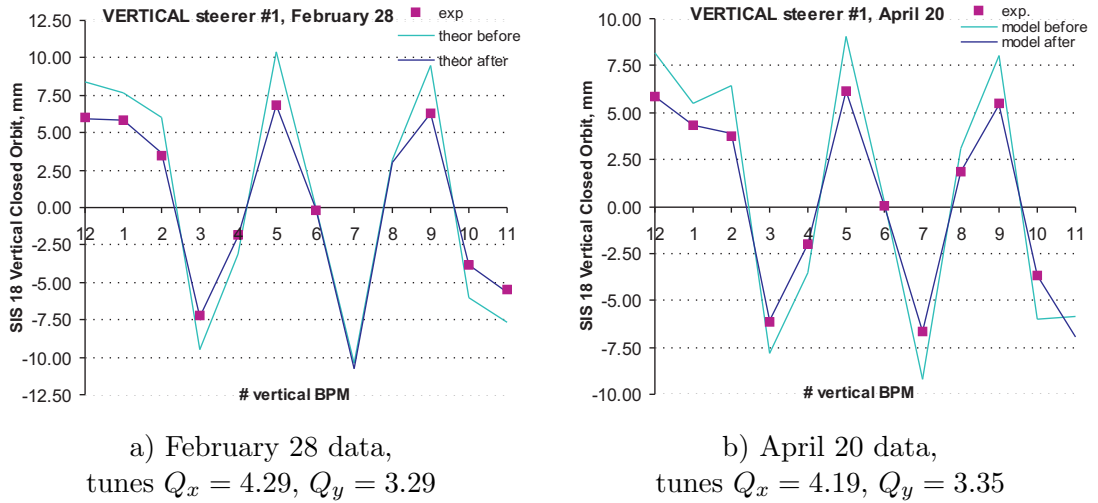


Figure 6: Measured and model response from the vertical steerer #1 (S01KM2DV) at 12 BPMs: a) February 28 measurement: BPMs #7 (S07DX) and #8 (S08DX) are missing; b) April 20 measurement: BPM #11 (S11DX) is missing.

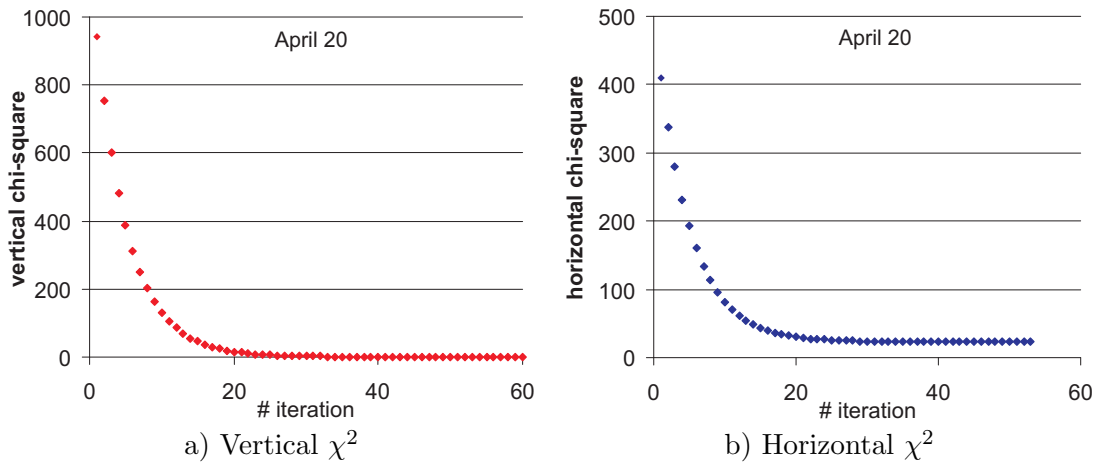


Figure 7: χ^2 normalized by number of data points vs. number of iterations calculated by Levenberg-Marquardt method for the vertical ORM a) and by SVD for the horizontal ORM b), both measured on April 20.

4 Data analysis

After the above algorithm has been tested as described in the previous Section, we apply it to calibrate ‘real’ quadrupole gradients, BPMs and steerers of the SIS18. Fig. 6 shows very good agreement between the measured and model response for one of the vertical steerers after the fit. In Fig. 6 is shown the ‘model before’ obtained with MAD for the vertical steerer #1 (S01KM2DV) before ORM fit applied. The ‘model after’ is a MAD simulation for the same steerer taking into account the retrieved fit parameters (vertical BPM and steerer calibration factors, quadrupole gradient errors). The convergence of

the χ^2 normalized by number of data points for the vertical and horizontal ORM (April 20 measurement) is presented on Fig. 7.

4.1 Error analysis: random and systematic errors

Next we discuss if these model parameters are really those of SIS18. Both random and systematic errors of the ORM measurements have to be addressed. The simplest way to find out how much the fitted parameters vary due to random errors in the measurements is to take several data sets, analyze each one separately, and see how much the fitted parameters vary for the different data set [11]. The SIS18 ORM has been measured three times, and fitted to a model for each response matrix. Then for each parameter the average over the three data sets was calculated together with the standard deviation, see Tables 5, 6, 7. The numbers from the tables are visualized on Figs. 8, 9, 10, 11. Note that Table 7 represents not the averaged fitted quadrupole gradients q^{orm} , but the averaged quadrupole errors Δq_l that should be added to the nominal values q^{nom} of Table 3 according to the following equation: $\Delta q_l = q^{\text{orm}} - q^{\text{nom}}$. The retrieved from ORM fit BPM and steerer calibration factors (Tables 5, 6) connect measured and model response matrices via $M_{ij}^{\text{model}} = M_{ij}^{\text{data}} / (g_i f_j)$ according to Equation 4.

Table 5: Calculated vertical BPM and steerer calibration factors averaged over three data sets and their standard deviations.

BPM	calibration g_i	st. dev. %	steerer	calibration f_j	st. dev %
S01DX	0.67	0.019	S01KM2DV	0.98	0.048
S02DX	0.65	0.032	S02KM2DV	0.98	0.031
S03DX	0.70	0.018	S03KM2DV	0.98	0.051
S04DX	0.68	0.034	S04KM2DV	0.99	0.028
S05DX	0.63	0.024	S05KM2DV	0.95	0.032
S06DX	0.69	0.035	S06KM2DV	0.96	0.030
S07DX	0.70	0.023	S07KM2DV	0.98	0.038
S08DX	0.61	0.024	S08KM2DV	0.99	0.012
S09DX	0.63	0.021	S09KM2DV	0.98	0.032
S10DX	0.67	0.033	S10KM2DV	1.01	0.005
S11DX	0.66	—	S11KM2DV	0.67	0.024
S12DX	0.70	0.042	S12KM2DV	1.00	—

To evaluate how good the fit is, it is useful to normalize χ^2 by the number of data points N , see Table 8. The minimum χ^2 normalized by the number of data points N is taken as a criteria of the fit quality and defined as follows [11]

$$\chi_{\text{min per data point}}^2 = \frac{\chi_{\text{min}}^2}{N_{\text{data points}}} \simeq 1 \quad (18)$$

$\chi_{\text{min per data point}}^2 \simeq 1$ indicates that errors in the fitting are of the order of random errors [11, 9, 10]. Statistically for the randomly distributed errors the test of the minimum χ^2 per data point for $N \simeq 120$ can not exceed 1.4. In Table 8 the minimum χ^2 s per data point and the total numbers of data points of the three measurements are presented. The vertical minimum χ^2 per data point of the February 28 measurement is large compared to the April measurements, for which the minimum χ^2 s per data point are centered around 1.0. The value 13.98, several standard deviations above 1.0, could

Table 6: Calculated horizontal BPM and steerer calibration factors averaged over three data sets and their standard deviations.

BPM	calibration g_i	st. dev. %	steerer	calibration f_j	st. dev %
S01DX	0.98	0.149	S01MU1A	1.14	0.065
S02DX	0.97	0.064	S03MU1A	1.06	0.084
S03DX	0.80	0.008	S05MU1A	1.16	0.007
S04DX	0.92	0.029	S06MU2A	1.0	0.000
S05DX	0.39	0.025	S09MU1A	1.15	0.056
S06DX	1.06	0.021	S12MU1A	1.18	0.023
S07DX	0.86	0.062	—		
S08DX	0.98	0.007	—		
S09DX	0.68	0.017	—		
S10DX	0.92	0.018	—		
S11DX	0.97	0.045	—		
S12DX	0.93	0.042	—		

Table 7: Calculated horizontal (horizontal focusing) and vertical (vertical focusing) quadrupole gradient errors averaged over three data sets and their standard deviations.

horizontal quadrupole index	gradient error, in units $10^{-3} (m^{-2})$	st. dev., in units $10^{-3} (m^{-2})$	vertical quadrupole index	gradient error, in units $10^{-3} (m^{-2})$	st. dev., in units $10^{-3} (m^{-2})$
S01QS1F	4.066	3.020	S01QS2D	1.815	0.316
S02QS1F	-2.718	3.121	S02QS2D	0.093	0.432
S03QS1F	2.057	3.318	S03QS2D	0.889	0.158
S04QS1F	0.183	2.289	S04QS2D	1.834	0.716
S05QS1F	-2.705	0.676	S05QS2D	1.494	0.580
S06QS1F	4.473	5.116	S06QS2D	0.912	0.210
S07QS1F	-4.248	1.959	S07QS2D	1.239	0.367
S08QS1F	10.014	6.043	S08QS2D	-0.374	0.542
S09QS1F	2.036	2.813	S09QS2D	2.075	0.803
S10QS1F	-1.853	0.566	S10QS2D	0.856	0.428
S11QS1F	-2.181	7.365	S11QS2D	-1.537	0.211
S12QS1F	6.710	4.322	S12QS2D	1.124	0.097

be explained as the fact that orbit measurement errors were not normally distributed and there is a contribution of systematic errors to the February 28 result. However, in the results of February 28 the vertical data fit agree well with the other two data fits, see Figs. 8, 10. The agreement of all three vertical data fits within rms deviation of several % indicates the uniqueness of the retrieved vertical model.

The horizontal minimum χ^2 s per data point all are not very satisfactory, see Table 8. The reason for that is due to random and systematic errors. The first reason is the relative lower accuracy in the measurements of horizontal beam position. The rms uncertainty σ_{ij} of horizontal orbit response has an average value ~ 0.2 mm/mrad (~ 200 μ m/mrad). The experimental horizontal ORM has gotten many small eigenvalues that correspond to noise in the data. To solve this problem, we use the SVD method for the χ -square minimization, and apply the tolerance threshold to remove the singularity.

Table 8: χ^2 statistics from three ORM vertical data fits.

Experiment	minimum vert. χ^2 per data point	minimum hor. χ^2 per data point
February 28	13.98 ($N_{\text{vert}} = 120$)	3.30 ($N_{\text{hor}} = 60$)
April 8	1.19 ($N_{\text{vert}} = 132$)	19.02 ($N_{\text{hor}} = 72$)
April 20	0.74 ($N_{\text{vert}} = 132$)	23.17 ($N_{\text{hor}} = 72$)

As discussed in Sec. 2.2, it is important to choose a proper threshold of singular value rejection (tolerance level). cutting out too many eigenvalues will make the solution space incomplete and solution will suffer, leaving in too many small eigenvalues will make the solution unstable. The selected tolerance level was set to eigenvalue ~ 0.05 .

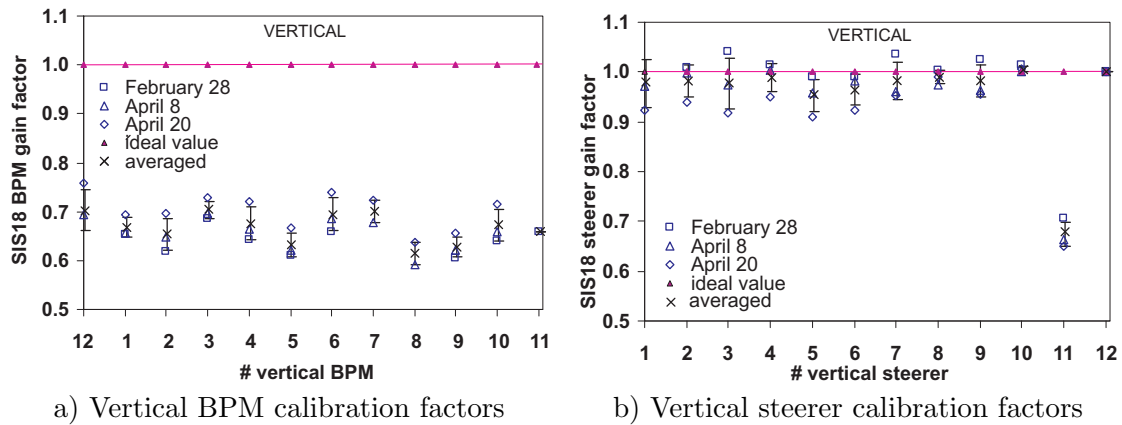


Figure 8: Vertical BPM a) and steerer b) calibration factors obtained from SIS18 ORM fit.

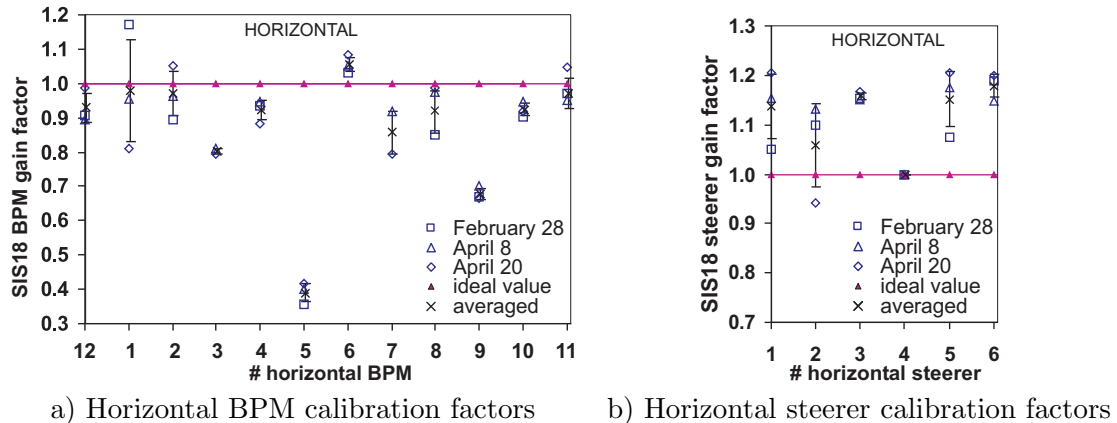


Figure 9: Horizontal BPM a) and steerer b) calibration factors obtained from SIS18 ORM fit.

Another important question is wherever the accuracy of the horizontal position measurement is good enough for the fit to produce a model that uniquely represents the synchrotron. Comparing the results of the three separate fits is possible to estimate the accuracy and the uniqueness of the resulting model. The difference between these three quadrupole gradient errors' fits using all 24 quadrupoles in the fit achieved more than 40%. This suggests for the present measurement accuracy that the number of quadrupoles used in the fit is too large. Foreseeing this problem, only half of the 24

focusing quadrupoles were allowed to be varied for the fitting. The variation between the fits is much smaller than for the case of all 24 quadrupoles. This is an indication that quadrupole variables can degenerate, i.e. the data does not provide enough information for a unique set of quadrupole errors. The number of quadrupoles in the fit has to be reduced [18]. The exclusion of some quadrupoles in the fit will increase the systematic errors in the considered model parameters. Therefore, another source of the systematic errors comes from not considering in the orbit response other model parameters, which do contribute to the experimental response data. In the horizontal fit model parameters also dipole gradient errors were excluded, because of lack of data points ($N = I \times J$), see Table 8. For the horizontal ORM measurement only 6 steerers were available for use, that is not sufficient to resolve the fit of all desirable parameters. The not considered 24 dipole gradient errors and 12 focusing quadrupole gradient errors do contribute as systematic errors into the high final horizontal χ^2 , see Table 8.

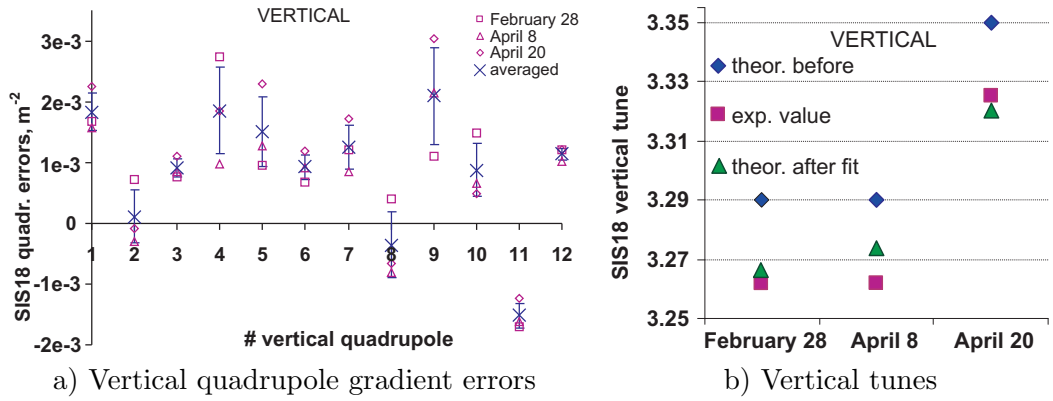


Figure 10: a) Vertical quadrupole gradient errors, obtained from SIS18 ORM fit; b) vertical measured and given tunes before and after the ORM fit.

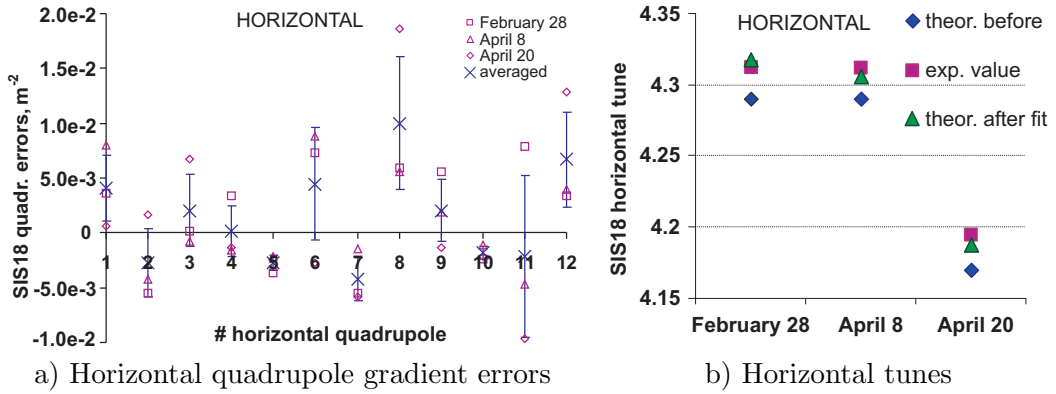


Figure 11: a) Horizontal quadrupole gradient errors, obtained from SIS18 ORM fit; b) horizontal measured and given tunes before and after the ORM fit.

4.2 Discussion on the results: measurement and model predictions

Next we discuss the retrieved values of BPM, steerer calibration factors and quadrupole gradients. The dispersion function of SIS18 was not measured and was not considered in ORM to decouple BPM and steerer calibration factors. For this reason the BPM \mathbf{g} and steerer \mathbf{f} calibration factors have to be calibrated relatively to one steerer (see Sec. 2.1).

11 vertical steerers and 12 vertical BPMs were calibrated respectively to the vertical steerer #12 (S12KM2DV), see Table 5. 5 horizontal steerers and 12 horizontal BPMs were calibrated relatively to the horizontal steerer #6 (S06MU2A), see Table 6. The calibration factors for S12KM2DV and S06MU2A were set to 1.0 in the modelling. The calibration factors of these steerers have been checked manually during CO correction campaign February-March 2006 [4] by applying a local bump condition in order to be sure that this assumption is acceptable. The vertical BPM #11 (S11DX) was absent in two out of three measurements therefore there is zero standard deviation for it in Table 5.

The Fig. 8 a) shows that SIS18 vertical BPM calibrations are centered not around 1.0, but around 0.7. The horizontal BPM calibrations are lowered in $\sim 10\text{-}15\%$ as well. The reason for which the horizontal BPM #5 (S05DX) has $\sim 60\%$ lowered calibration factor has still to be understood. The BPMs are the so called ‘shoe-box type’ Beam Position Monitors [7], which measure the center mass of the beam. The SIS18 BPMs, see Fig. 12, have larger aperture in horizontal than in vertical plane for the construction reason of SIS18 chamber. The horizontal and vertical directions in each BPM are treated independently according to formulas

$$\begin{aligned} x &= K_x \cdot \frac{\Delta U_x}{\sum U_x} + \delta_x \\ y &= K_y \cdot \frac{\Delta U_y}{\sum U_y} + \delta_y, \end{aligned} \quad (19)$$

where the difference of voltages of the plates ($\Delta U_x, \Delta U_y$) is normalized to their sum ($\sum U_x, \sum U_y$); K_x, K_y are pick-up constants; δ_x, δ_y are pick-up offsets. For the simulated SIS pick-up the value are: $K_x = 226$ mm, $K_y = 62.7$ mm, $\delta_x = -4.8$ mm, $\delta_y = +0.39$ mm [7]. In Ref. [7] is noticed that the values K_x and K_y obtained in the simulations are 20% larger than the experimental values measured with the test set up. The pick-up constants K_x and K_y can be changed for each BPM, the POSI data then will be updated automatically [20].

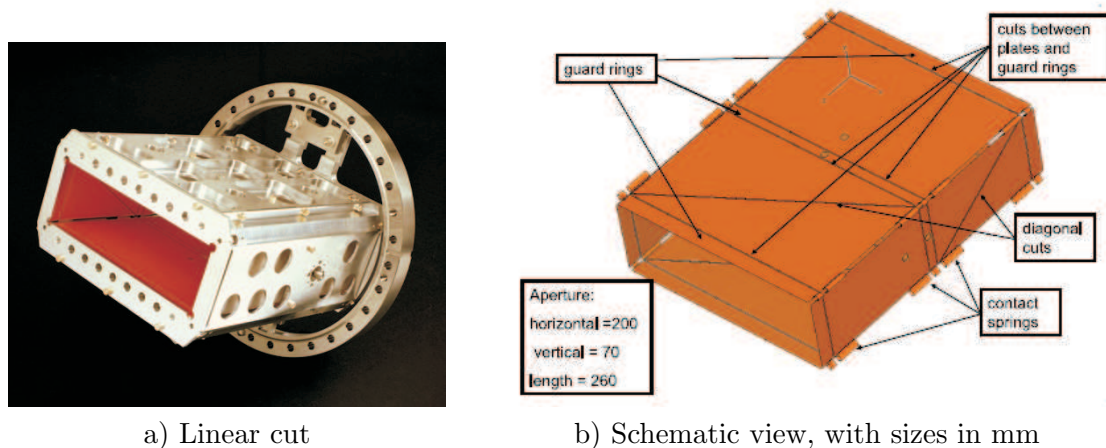


Figure 12: View of the SIS18 BPMs.

As the CO correction by local bump method was possible, all steerers were expected in

general to be well calibrated, except for one or two, see Fig. 3. The vertical steerer calibrations retrieved from the ORM model are centered around 1.0 except for the steerer #11 (S11KM2DV) that has calibration factor only 0.7 and seems to be responsible for ‘imperfect’ local bump on Fig. 3 b). A check of the #11 (S11KM2DV) has been done and the lower magnetic field in $\sim 30\%$ has been found [22]. The reason for that is not a device malfunction, but a construction different design: the steerer has larger aperture. Nevertheless, as its’ calibration factor is different to the other steerers, it destroys the correction done by the other steerers. The steerer #11 (S11KM2DV) has to get a new calibration factor 33% higher in the SIS18 control program to be used in the CO correction by local-bump method.

As it was noticed in the introduction there are 36 quadrupoles in the SIS18: 24 horizontal focusing quadrupoles and 12 vertical focusing quadrupoles, which form five families. In Table 3 the nominal values of the SIS18 quadrupole gradients are presented. The values of quadrupole gradients are the currently used in the SIS18 lattice model for simulations in MAD [15] and MIRKO [8] are proper adjusted [4]. Therefore, the quadrupole errors are expected to be not too high in average $\sim 0.1\text{-}0.3\%$ of the nominal values, see Tables 7, 3. It is well known at GSI that the SIS18 tune has a systematic tune shift from the one set in SISMODI. Simulations made with the retrieved quadrupole gradient errors (Table 7) bring the model tune closer to the measured value, see Figs. 10 b), 11 b).

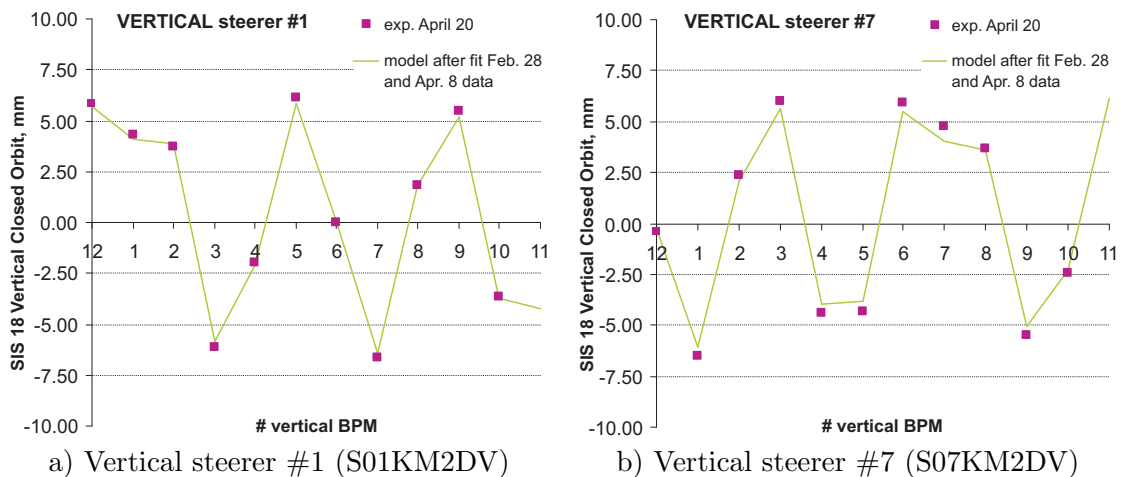


Figure 13: The comparison: the ORM model deriving from the measurements February 28 and April 8 is correlated with the measurement of April 20.

The crosscheck wherever the fitted model parameters are correct is made by comparing them with the SIS18 data that were not used in the model fitting. As we made ORM measurement at two different tunes, see Table 4, the following test was performed: the ORM model deriving from two measurements for the tune (4.29; 3.29) is used to predict the measurement for the tune (4.17; 3.35). The quadrupole gradient errors were retrieved from two measurements for the tune (4.29; 3.29) and then modelled in MAD. The model MAD matrix multiplied by BPM and steerer calibrations retrieved from the same two measurements is able to fit the measured matrix for the tune (4.17; 3.35). Fig. 13 shows the measured and the deriving from two measurements model response from two different vertical correctors. Using the model parameters deriving from two measurements the initial vertical χ^2 normalized by number of data points has been

reduced from 942.03 to 40.89.

5 Conclusion and Outlook

- The ORM analysis provided the detailed information on the SIS18 linear optics. Three ORM were fitted to calibrate horizontal and vertical BPMs, steerers and quadrupole gradients.
- The results of the three vertical fittings are in agreement, that indicates the uniqueness of the found vertical fit model for the SIS18.
- The fitted values of the quadrupole gradients, BPM and steerer calibrations provide the optimized lattice model as well as hints of device malfunctions.
- The ORM modelling gives 33% lower calibration factor for vertical steerer #11 (S11KM2DV). For this steerer it was found that its magnetic field is $\sim 30\%$ weaker than expected, as predicted by ORM analysis. This steerer needs a correction in the control program. Therefore its effect becomes equal to those of the other steerers.
- The present vertical calibration of all BPMs should be increased in $\sim 25\text{-}30\%$ according to the ORM modelling results.
- The present horizontal BPM calibration is also lowered down in $\sim 5\text{-}10\%$ according to the ORM predictions. The present horizontal steerer calibration is in $\sim 10\%$ higher than 1.0.
- The present low accuracy of the horizontal beam position led to high systematic and random errors in the measured horizontal response matrices. The present accuracy of the horizontal measurements does not allow to uniquely define all 24 focusing quadrupole errors in the ring and brings large error bars in the fit of other parameters. It was possible to define uniquely only 12 horizontal focusing quadrupole errors. The horizontal accuracy should be improved at least to the same value as the vertical one. From an horizontal orbit response of better quality, a better model of the SIS18 with many more fit parameters can be retrieved.
- The found quadrupole gradient errors reproduce the systematic tune shift observed experimentally.
- The 6 horizontal steerers used at the moment are too few parameters for the horizontal ORM modelling (not enough data points). To better resolve the horizontal data at least 12 steerers are needed: one in each period.
- The dispersion was not measured in the SIS18 ORM experiments here discussed. The dispersion measurement would be desirable in the future to provide more information for orbit response analysis.

6 Acknowledgments

We would like to thank I. Hofmann for his support on this work; P. Spiller and M. Kirk for help in experiments and in machine operation; B. Franczak and P. Schütt for their

advice and assistance; the diagnostics, magnet and BEL groups for technical support in particular P. Forck, P. Kowina, W. Kaufmann, J. Schölles, G. Fröhlich, C. Muehle; SIS18 operator team in particular U. Scheeler, C. Wetzler.

References

- [1] G. Franchetti, T. Giacomini, M. Kirk, A. Parfenova, "Resonance Induced Beam Loss in SIS18", GSI-Acc-Note-2005-12-001, GSI, Darmstadt, Germany, pp.11, <https://www.gsi.de/onTEAM/beschleuniger/notizen/public/GSI-Acc-Note-2005-12-001.pdf>.
- [2] X. Huang, S.Y. Lee, Eric Prebys, Chuck Ankenbrandt, "Fitting the Fully Coupled ORM for the Fermilab Booster", <http://lss.fnal.gov/archive/2005/conf/fermilab-conf-05-115-ad.pdf>.
- [3] A. Parfenova, G. Franchetti, B. Franczak, M. Kirk, C. Omet, A. Redelbach, "Using Local Bumps for correcting the SIS18 Closed Orbit", GSI Annual Reports 2006, GSI, Darmstadt.
- [4] A. Parfenova, G. Franchetti, B. Franczak, M. Kirk, C. Omet, "SIS18 closed orbit correction using a local bump method", GSI-Acc-Note-2006-11-001, GSI, Darmstadt, Germany, <https://www.gsi.de/onTEAM/beschleuniger/notizen/public/GSI-Acc-Note-2006-11-001.pdf>.
- [5] S.Y. Lee, "Accelerator Physics" Second Edition, World Scientific Publishing Co. Pte. Ltd. 2004, pp.124.
- [6] A. Redelbach, CO-Korrektur mit MIRKO bzw. SIST (2006), \\Winfilesva\scratch\Redelbach\Documents\COC\Auto_COC.pdf.
- [7] P. Kowina, W. Kaufmann, J. Schölles and M. Schwickert, "Optimization of "Shoebox type" beam positions monitors using the finite element method", in Proc. DIPAC-2005, pp. 114, Lyon, France, http://www-bd.gsi.de/conf/dipac05/dipac05_kowina.pdf.
- [8] B. Franczak, private communication.
- [9] I.N. Bronshtein, K.A. Semendyayev, G. Musiol, H. Muehlig, "Handbook of mathematics" 4th Edition, Springer 2004.
- [10] Numerical recipes in C: the art of scientific computing, <http://www.nr.com>.
- [11] J. Safranek and M.J. Lee, "Calibration of the X-Ray Ring Quadrupoles, BPMs, and Orbit Correctors Using the Measured Orbit Response Matrix", Proceedings of the 1994 European Particle Accelerator Conference, pp. 1027.
- [12] J. Safranek, "Experimental determination of storage ring optics using orbit response measurements", Nuclear Instruments and Methods in Physics Research, 1997, pp. 27.
- [13] Effective AWK Programming, <http://www.gnu.org>.

- [14] <http://www.scilab.org>.
- [15] H. Grote and F.C. Iselin, The MAD Program (Methodical Accelerator Design), Version 8.1, User's Reference Manual, CERN/SL/90-13(AP)(1991), <http://mad.web.cern.ch/mad/>.
- [16] <http://en.wikipedia.org/wiki/Aliasing>.
- [17] <http://bel.gsi.de/mk/operating/posi/posi.html>.
- [18] V. Sajaev, V. Lebedev, V. Nagaslaev, V. Valishev, "Fully coupled analysis of orbit response matrices at the FNAL TEVATRON", Proceedings of Particle Accelerator Conference, Knoxville, Tennessee, pp. 3364.
- [19] P. Forck, Joint University accelerator school "Lecture Notes on Beam Instrumentation and Diagnostics", GSI, <https://www-bd.gsi.de/conf/juas/juas.html>.
- [20] P. Forck, W. Kaufmann, P. Kowina, private communication.
- [21] G. Franchetti, B. Franczak, and P. Schütt, GSI Note GSI-Acc-Note-2004-05-001, GSI, <https://www.gsi.de/gsitools/>.
- [22] C. Muehle, GSI magnet group, private communication.